KnE Engineering

Knowledge E
enriching | engaging | empowering

Conference Paper

Matlab® Algorithm to Simulate the Dynamic Behavior of an NiTi Alloy through Ansys® APDLTM Models

Jean César Hilário[1], Manuel Braz-Cesar[1], Carlos Andrade[1], and Adailton Silva Borges[2]

[1]Polytechnic Institute of Bragança
[2]The Federal University of Technology – Paraná

Corresponding Author:
Jean César Hilário
a39513@alunos.ipb.pt

🔓 **OPEN ACCESS**

Abstract

In recent years, technological advances related with the so-called intelligent materials have been exploited for problem solving in many engineering fields. In this regard, shape memory alloys (SMA) seem suitable for medical and engineering applications and many others. These alloys have the ability to return to the original form after an apparently plastic deformation by applying heat and the also ability to perform phase changes with voltage variations under a specific temperature. These properties allow the development of a hysteretic loop with energy dissipation, which can be used as a damping element in a vibratory system. In this paper, a MATLAB algorithm was developed to create an interface with the Ansys® APDL™ software that simulate the dynamic behavior of a SMA. The software is capable to obtain the cyclical behavior of a vibratory mechanical system based on the energy dissipation properties of the SMA. The results show that the free vibration of a mass-damper (alloy) system presents the energy dissipation related in magnitude with the area of the hysteresis loop until the deformation caused by the motion which does not correspond to a voltage required to initiate the (direct) phase transformation of the material, thus reducing the displacement to a constant level.

Keywords: SMA, ANSYS APDLTM, Matlab

1. Introduction

Intelligent materials have brought great development opportunities, since this kind of material have the coupling of multiple physical domains, i.e., variations in non-mechanical properties, such as temperature and magnetic field, cause variations in mechanical properties (on a larger scale than noticeable changes in common materials) [1, 2].

Shape memory materials or alloys (SMM or SMA) are allocated in this category, where changes in the material temperature field cause changes in mechanical properties. More specifically, they are characterized by two unique features: recovering their original

shape from a seemingly plastic strain by raising the temperature thereof and having a hysteresis loop in the stress-strain diagram [3].

These properties arouse interest in several application areas, mainly in energy dissipation during seismic phenomena (earthquakes), so that some works are developed to prove and disseminate information on how SMA can be applied in order to stabilize as much as possible. the structure to decrease the amount of damage [4–8].

Natural phenomena are random, and the prediction of how and when they will occur is extremely difficult. In addition to earthquakes, wind is responsible for acting on structures that can generate vibrations, so studies such as those proposed in [9] are essential in order to reduce the damage that can be caused.

Applications with SMA are generally used in a temperature range where the alloy remains in two distinct phases, austenite (phase present at high temperatures) and martensite (phase that occurs at low temperatures). In order to facilitate the identification of transformations, the term direct transformation is used when the initial phase is austenitic and the final martensitic, while reverse transformation is the opposite way [1].

The direct and reverse transformations have their beginning and end defined by characteristic temperatures, being M_s and M_f for the initial and final temperatures of the direct transformation and A_s and A_f for the reverse transformation respectively. More details on the mentioned transformations can be found in [1, 3].

The relationship of characteristic transformation temperatures to transformation stresses is given by considering the stress-temperature diagram in Figure 1, where stresses are calculated by the ratio of material parameters: angular coefficients for martensite (C_M) and austenite (C_A) and the initial and final critical transformation stresses [10] listed in Equations 1, 2, 3 and 4.
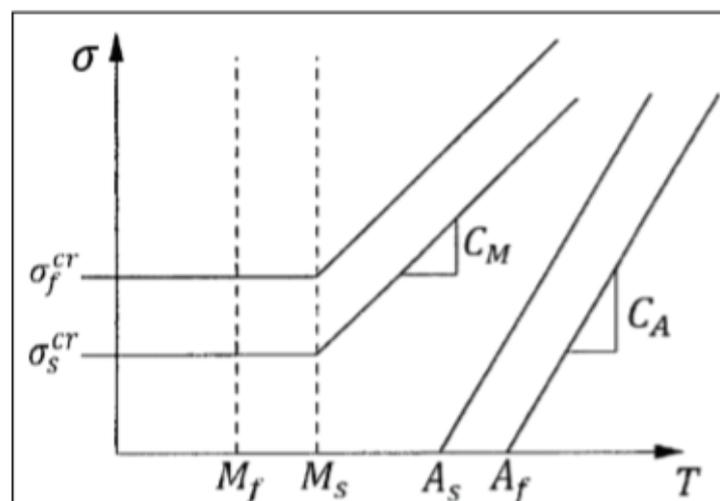
Figure 1: Stress-temperature diagram for identifying characteristic properties [11]

$$\sigma_s^{MA} = C_A \left(T - A_s \right) \tag{1}$$

$$\sigma_f^{MA} = C_A \left(T - A_f \right) \tag{2}$$

$$\sigma_s^{AM} = C_M \left(T - M_s \right) + \sigma_s^{crit} \tag{3}$$

$$\sigma_f^{AM} = C_M \left(T - M_s \right) + \sigma_f^{crit} \tag{4}$$

where "σ" is the stress in material [Pa], "C" is the angular coefficient of the stress-temperature ratio [Pa/K], "T" is the room temperature [K], "A" the direct transformation temperature [K], "M" the reverse transformation temperature [K], the subscribers "s" and "f" indicate respectively the initial and final stages of the transformations, "A" and "M" represent the phase of the material, in the order presented austenite and martensite, the superscripts "AM" and "MA" following are indications of the forward and reverse transformations and "crit" represents a critical property value required for the martensitic transformation.

Among the mentioned characteristics of SMA, the present work will focus on superelasticity (a phenomenon characterized by a hysteresis loop in the stress-strain curve, which tends to occur when mechanical loading is applied and removed while temperature is maintained above A_f) [3].

The current research presents a study of the cyclic tensile and compressive behavior of a vibratory system under hysterically damped free regime condition enhanced by the consideration of change in transition temperatures that occur during the alloy training process.

2. Mathematical Modeling

In order to simulate the SMA, it is necessary to define a model that represents the unique behavior of these alloys through several applications. Since its discovery as intelligent material, several researchers have proposed mathematical considerations and models to be used in simulations, some of which have been developed by [10–12].

In order to facilitate the analysis of the considerations adopted by the software Ansys®, an elementary division of the necessary considerations will be used to elaborate a constitutive model, being the mechanical, the kinetic and the thermal laws.

Mechanical laws are responsible for relating the stress-strain behavior of the alloy and are necessary due to the condition that SMA is a type of material that acts by

changing the crystal structure, and that this change is not instantaneous throughout the structure of the alloy. The second type of law to be considered is the kinetic law, which is responsible for describing the way internal transformations occur, i.e., what influence variables such as stress and strain have on the change between phases of the material.

The thermal model can be considered negligible in situations where the application of the alloy is based on a quasi-static case, where the heat exchange between the material and the environment can be neglected. For dynamic studies, when considering a high application rate and load removal, a high amount of generated energy is expected and if the system is not designed to dissipate this energy, an increase in material temperature will occur, requiring this is considered in simulations.

The model to be detailed in this paper is the one used by Ansys® APDL^{TM}, where an isothermal consideration will be performed. Superelasticity (SE) simulation does not consider martensite reorientation, only direct and reverse transformations. The deduction of the mathematical equations used by the software to describe the material behavior can be found in [12].

The mechanical vibratory system to be analyzed is shown in Figure 2. This consists of a mass connected to a circular bar of nitinol (one of the most well-known SMA today) that is built into one end.
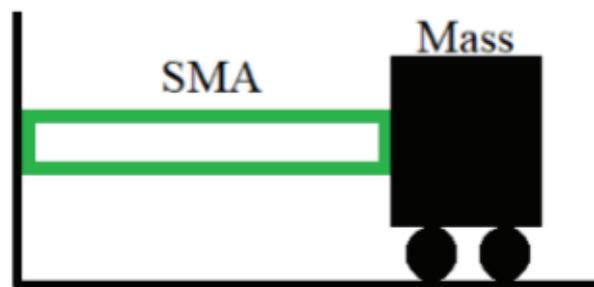
Figure 2: Mechanical Vibratory System.

From Figure 2, it is noted that the SMA is a combination of stiffness and damping thereof. This is due to the interest in analyzing only the property that SMA has to dissipate energy. For these analyzes, the equations present in the standard vibration literature [14, 15] for hysterically damped systems will be used. Therefore, Equation 5 is fundamental to the movement to be studied.

$$ma + cv + kx = 0 \tag{5}$$

where "m" is the mass [kg], "c" is the viscous damping coefficient [Ns/m], "k" is the stiffness coefficient [N/m], "a" is the acceleration [m/s^2], "v" is the speed [m/s] and "x" is the displacement [m] of the system.

The resolution of this equation and the considerations for hysteretic damping analysis can be found in the references mentioned and will be omitted in the present work. The resolution of this equation and the considerations for hysteretic damping analysis can be found in the references mentioned and will be omitted in the present work. In order to summarize the deductions, SMA presents a hysteresis loop in the force-displacement diagram and consequently in the stress-strain. This loop is responsible for dissipating energy that provides a hysteretic damping constant. With this constant and the stiffness of the system, an equivalent viscous damping coefficient is determined in order to facilitate the analysis. Applying this to the solution of Equation 5 gives the system response.

In cases of free vibration, the response of the system is directly linked to the initial conditions of the system, which are displacement and velocity. For the present simulation, the system will be subject to an initial condition of pure displacement.

Since the damping of the system is by hysteresis, the energy dissipation will be done only on unloading. In this way, the initial simulation in Ansys® with the geometric model, the boundary conditions and the initial conditions that will result in the stress-strain diagram for the initial displacement provided is made. Considering that the specimen is pulled to the set value and released to return to the equilibrium position, i.e. a residual deformation equal to zero.

The motion equation solution given above is used having the equivalent damping and stiffness value calculated from the diagram provided in the simulation output. This motion would be processed to a zero strain value, as provided by the software, however, on the assumption that the only form of system energy dissipation is during the hysteresis loop, an extrapolation of the motion is made so that the graph of the vibration reaches the next peak (in this case negative), because until that point there is no formation of the loop.

The negative peak value is then used as the new initial condition input in Ansys®, where the simulation is redone for a compression. This new simulation will provide the same output variables that will be used to determine the dissipated energy during the movement from equilibrium (zero deformation) to the compression peak and back to equilibrium (these are the steps followed by the software during the simulation). Again, the equation of motion is extrapolated, this time to the next traction peak, whereas there is no energy loss during loading, it is the value that the system tends to approach, which is then used in the next simulation.

These steps are repeated so that the system uses the stress-strain diagram in conjunction with the solution of a motion equation for a hysteretic damping case to account for energy losses as system behavior changes over time.

The deduction mentioned above consists of the calculations performed by Ansys® so that the material behavior is usually obtained under a static analysis condition. In order to simulate its dynamic behavior (similar behavior to those obtained in [16, 17]), a series of improvements were developed by [18] in order to update the material properties as it is subjected to a cyclic movement (experimentally studied in [19]). The main phenomena that led to the development of the equations considered in the present work are:

(1) The initial and final direct and reverse transformation voltages decrease as the cycle number increases during the load-unload process when subjected to constant temperature; (2) The above transformation temperatures are elevated as the number of cycles increases during constant voltage heatingcooling processes; (3) The start and end lines of the forward and reverse transformations in the voltage-temperature plane move in the direction of low voltage and high temperature as the cyclic loading progresses; (4) Permanent deformation increases as cyclic deformation progresses; (5) Transformation strain range decreases with increasing number of cycles; (6) The above mentioned phenomena vary significantly in the early cycles, however the level of variation in each characteristic decreases as the number of cycles increases.

The mentioned changes are part of the training process cited by [1] where it refers to the condition of repeatedly applying cyclic loading on the material to a point where the hysteretic response present in the stress-strain diagram stabilizes and the inelastic (or permanent) strain) is saturated.

Experimental results in [18, 20] allow confirmation of the phenomena related to a cyclic traction loading, which present changes in all the phenomena mentioned above, however for a case where loading involves traction and compression cycles, a study is needed. to identify the behavior of inelastic deformation, so that in the present work the updating of the mentioned characteristics focus only on the characteristic phase transformation temperatures.

Thus, these values must be updated between the simulation cycles that have been described. For the transformation temperatures one must be written as a function of the number of cycles as in Equations 6 and 7.

$$M_{s,f}(N) = M_{s,f}(0) + \alpha_M \{1 - e^{-\beta} M^N\} \tag{6}$$

$$A_{s,f}(N) = A_{s,f}(0) + \alpha_A \{1 - e^{-\beta} A^N\} \tag{7}$$

where $M_{s,f}(N)$, $A_{s,f}(N)$, $M_{s,f}(0)$ and $A_{s,f}(0)$ These are the initial and final transformation temperatures for the number of the cycle the load is in and the initial values of the materials. The coefficients α_M, β_M, α_A and β_A, as quoted in [18] "generally depend on material composition, production conditions, heat treatment for shape definition and cyclic loading conditions which are stress, strain and temperature levels".

Since it is necessary to repeat simulations, as well as to change the input parameters between each one of them including the need to perform parameter calculations where the previous simulation directly interferes with the next one, the algorithm is essential for the automation of the procedure. simulation, where Ansys® APDL^{TM} software is used as a solver for the case study.

The flowchart of Figure 3 graphically explains the algorithm cited to enable the simulation with the improvement of the dynamic behavior by changing the properties.
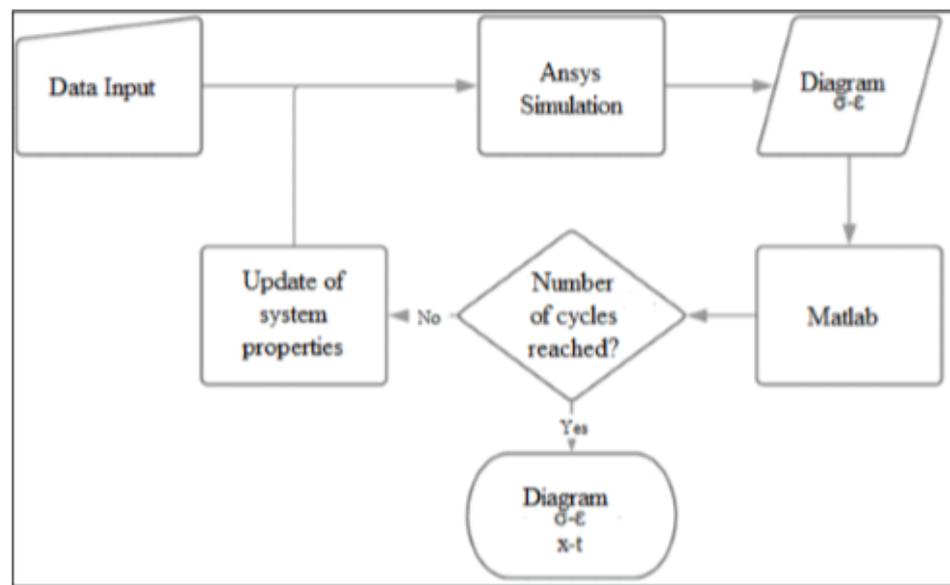
Figure 3: Algorithm flowchart

3. Numerical Simulation

Ansys® software must receive a few material properties to enable numerical simulation. These values are for generic properties the Poisson's ratio, the modulus of elasticity of the austenitic phase and specific for SMA, the initial and final stresses of the direct and reverse transformations, the maximum residual deformation and the correlation parameter regarding the tensile material responses. and compression, it is possible to observe in Table 1 the properties used according to the work of [21] for a Nickel-Titanium alloy called Nitinol.

TABLE 1: Material Properties

Material Property	Value
Poisson's ratio	0.33
Elasticity modulus - Austenite	67 [MPa]
Initial stress – Direct transformation	432.8 [MPa]
Final stress – Direct transformation	502.8 [MPa]
Initial stress – Reverse transformation	351.9 [Mpa]
Final stress – Reverse transformation	151.8 [MPa]
Maximum residual strain	0.067
Tensile-compression parameter	0

It should be noted that with the tensile-compression parameter considered zero, there is no difference in the results provided for these different load types. In order to disregard possible buckling effects that may occur, all simulations will be traction only.

Along with the definition of the material, the properties of the vibratory mechanical system are defined in Table 2, consisting of the geometric properties of the SMA bar, the mass attached to the end, the initial conditions and the environment.

TABLE 2: Dynamic System Features

Features	Value
Specimen radius	1 [mm]
Specimen length	10 [mm]
System attached mass	1 [kg]
Initial displacement	0.4 [mm]
Initial velocity	0 [mm/s]
Room temperature	60 [°C]

The finite element configured is SOLID186 and its basic definition according to [22] is a high order three-dimensional element that exhibits a quadratic displacement behavior. This element is defined as containing twenty nodes and having three degrees of freedom per node, being translations in the x, y and z directions. The element supports plasticity, hyperelasticity, creep, stress hardening, large deformations and the ability to undergo large deformations.

The finite element adopted is represented in Figure 4, where the option to be used is related to the model geometry, being defined during the mesh creation.

Mesh generation was done automatically using the software's own smart settings, using a refinement parameter "1", providing a quantity of 20.963 nodes, 14.085 elements
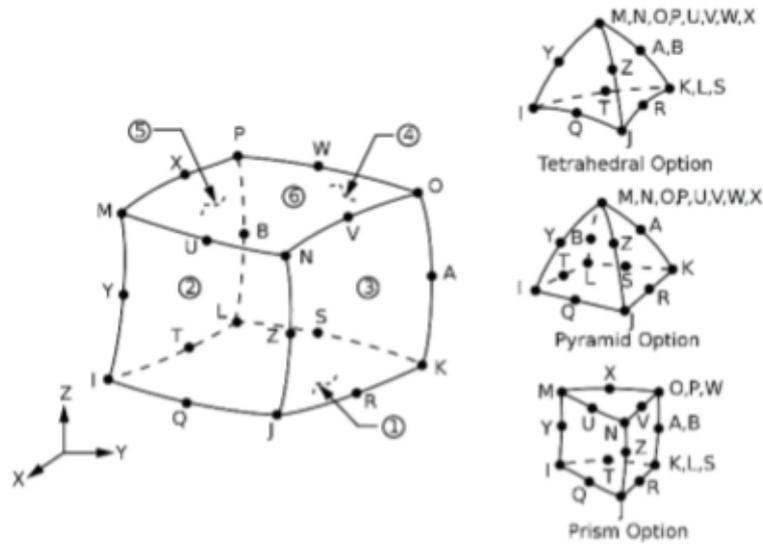
Figure 4: Finite element model adopted Fonte: [22]

and setting the tetrahedral option for the finite element format. The simulated model with the adopted mesh is represented in Figure 5.
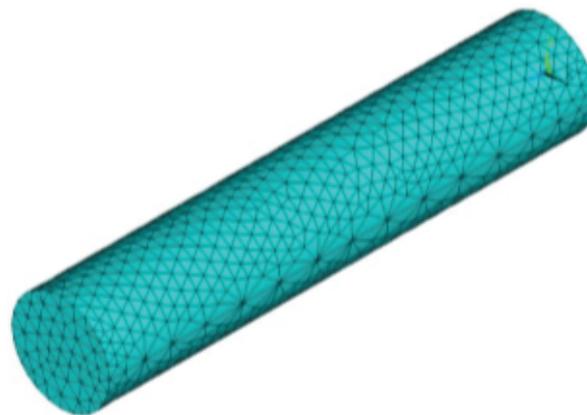
Figure 5: Template with defined mesh

Geometric boundary conditions consist of recessing one end of the beam to eliminate degrees of freedom and applying a linear displacement field to the other end. This displacement field is calculated by the software using the starting position at the equilibrium point, the maximum displacement to be reached and the final position (in this case, the equilibrium point) as the loading step. The Ansys solver has been configured via the "Sol'n Controls" option with the parameters given in Table 3.

Since the algorithm has been implemented to enable multiple traction or compression simulations to construct a dynamic chronology, it is responsible for making the changes in the maximum displacement mentioned above to match the next maximum peak provided by the vibration calculations for hysteretic damping.

The first simulation presents the results only for the dynamic behavior of 100 cycles, without considering the changes proposed by [18] for a cyclic loading case. The output data for the stress-strain diagram can be seen in Figure 6, where only cycles 1, 2, 5, 10, 20, 50 and 99 are plotted for easy viewing.

TABLE 3: Solution and Controls options

Parameter	Value
Analysis Options	Large Displacement Transient
Time step size	0.1
Mininum time step	0.05
Maximum time step	0.1
Full Transient Options	Ramped loading
Algorithm	Newmark algorithm
Application	High Speed
Equation Solvers	Program chosen solver
Nonlinear Options – Line search	On
Nonlinear Options –DOF solution predictor	Prog Chosen
Nonlinear Options –VT Speedup	Off
Equilibrium Iterations	1000
Cutback Control - Equiv. Plastic strain	0.15
Cutback Control - Explicit Creep ratio	0.1
Cutback Control - Implicit Creep ratio	0
Cutback Control - Incremental displacement	10000000
Cutback Control - Points per cycle	13
Cutback Control	Cutback according to ...

In the present diagram it is possible to observe that the amount of energy dissipated is much larger in the initial cycles and decreases as the amplitude of deformation decreases. According to Figure 7, the dissipated energy influences the dynamic behavior due to the reduction of the diagram area, and for the initial cycles, the reduction of the displacement is considerable, while when the hysteresis loop has a smaller area, the reduction is practically nil and the system can be considered as without damping.

It is noteworthy that from a given energy value that is being dissipated, vibration has a practically constant value, not reducing it to zero, as expected from a damped system. This effect proves the previously adopted condition where a hysteresis-damped system only has loop-dependent energy dissipation in the stress-strain diagram. From the point where the stress produced in the system by deformation is not enough to initiate phase
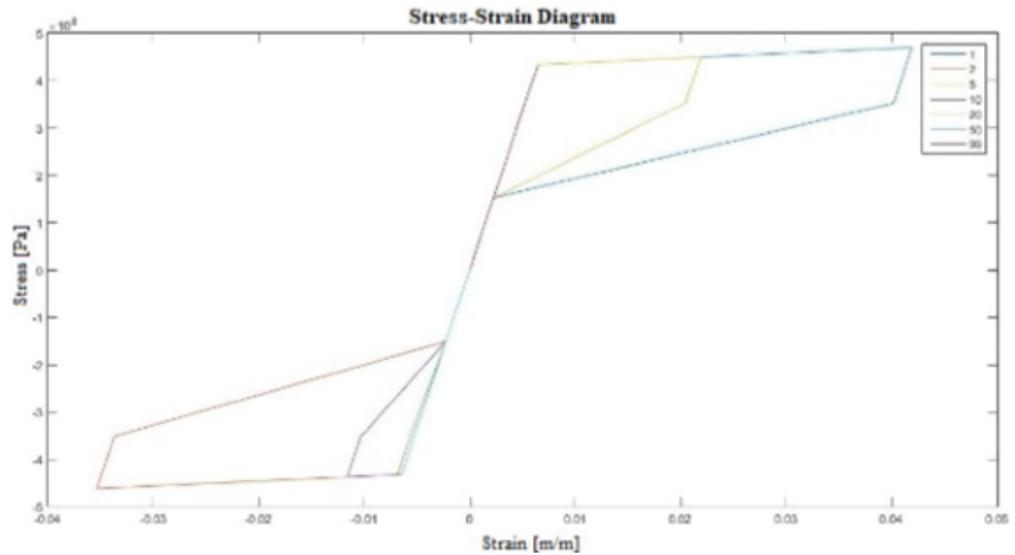
Figure 6: Stress-Strain Diagram for 100 simple cycles
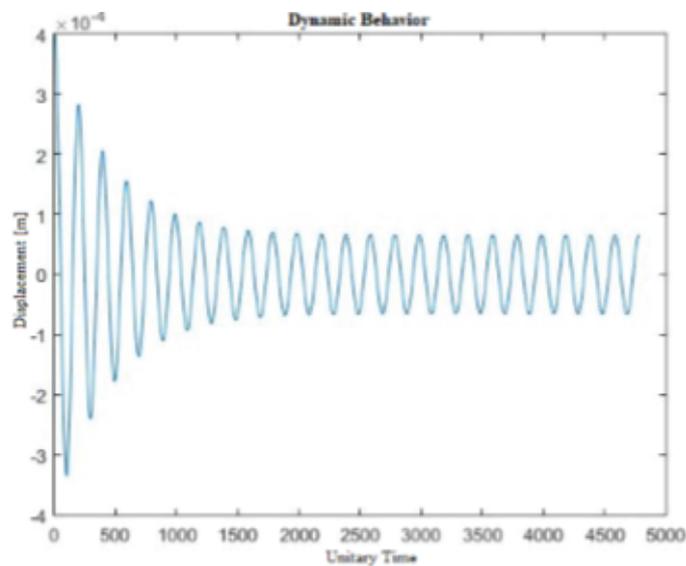
Figure 7: Dynamic Behavior without enhancement

transformation, the system does not dissipate energy and the deformation will remain constant.

In order to observe the training process of SMA during a direct application in free vibration, the equations extracted from the work developed by [18] were implemented in such a way that at each cycle the value of the transformation temperatures and consequently the stresses that from these are calculated to be updated and provided as input parameter to Ansys®.

The initial parameters were the same used for the simulation of simple cycles, providing as output data the stress-strain diagram that will be represented in Figure

8 considering the same cycles of the previous case as well as the dynamic response of the system present in Figure 9.
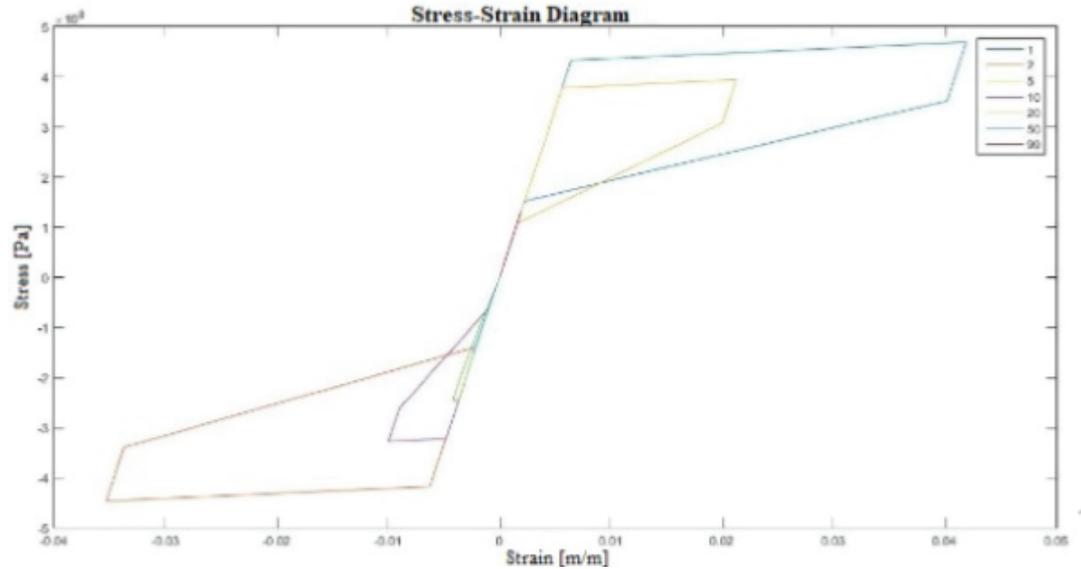
Figure 8: Stress-Strain Diagram for 100 enhanced cycles
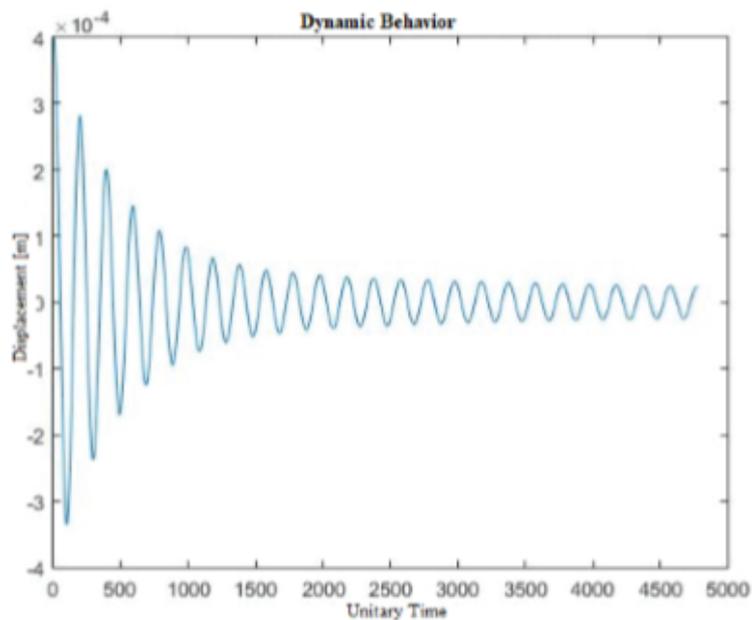
Figure 9: Dynamic Behavior with enhancement

4. Discussions

The observed dynamic behavior is consistent with the predicted vibration theory in the literature, whereby means of energy dissipation, a free vibration tends to reduce its amplitude while this damping system is present. This is observed in the graph shown

in Figures 7 and 9, where the amplitude of vibration decreases to the point where the voltage corresponding to the displacement is not sufficient to induce the transformation, i.e. the damping is inactive for the system, maintaining a amplitude of constant vibration. Taking the results of the dynamic graphs obtained for the algorithm without and with improvement of the transformation characteristics due to cyclic loading, we have that for the inactive damping condition the peak displacement value for the first case is close to 0.8 [mm], while for the second case it remains in the range of 0.3 [mm]. The main comparison is in relation to the improvement made through the proposed algorithm to include the changes due to cyclic loading in the LMF, where it is possible to observe a significant change between Figures 6 and 8. This change is responsible for altering the characteristic properties of the materials responsible for indicating phase changes (initial and final direct and reverse transformation temperatures), which change the behavior of the hysteresis loop (changing its area throughout the cycle), changing consequently the transforming voltage required to induce phase change (changes as the characteristic temperature changes, since both are related by equations 1, 2, 3 and 4) and therefore the maximum amplitude of vibration, since less voltage is required to induce phase transformation and therefore initiate the hysteresis loop for power dissipation.

5. Conclusions

The present work presented the considerations made to interconnect data provided for a loading-unloading cycle of a Nitinol bar with its dynamic behavior when subjected to an application from the results obtained for a three-dimensional dynamic model with a degree of freedom having as commercial Ansys® software to provide SMA behavior. Considerations have been implemented by other researchers to improve the dynamic simulations through the behavior of the alloys when subjected to traction-compression cycles, to allow a closer analysis of the actual behavior if the material has not undergone the training process. Regarding the dynamic data, the behavior observed was that of a damped system by the applied voltages induce or not the phase change. Thus, enabling the use of this type of material in dynamic applications whose objective is the dissipation of oscillations.

The implemented algorithm was able to provide data necessary for the design of dynamic applications involving the SMA as well as to predict the behavior to be expected if the material is subjected to the training process, since, as discussed, there is a change in the dynamic behavior of the SMA. can reduce the final swing amplitude by more than 50%. The importance of the algorithm is based on the need to perform

repetitive simulations by changing the dynamic boundary conditions as well as making the necessary calculations for the characteristic properties of the materials throughout each simulation.

References

[1] Lagoudas, D. C. (2008). *Shape Memory Alloys- Modeling and Engineering Applications*. New York: Springer.

[2] Sun, Y., Luo, J., Zhu, J. (2018). Phase field study of the microstructure evolution and thermomechanical properties of polycrystalline shape memory alloys: Grain size effect and rate effect. *Computational Materials Science*, vol. 145, pp.252-262.

[3] Silva, M. A. (2018). Simulação do comportamento dinâmico de sistemas mecânicos vibratórios amortecidos pelo comportamento pseudo-elástico de ligas com memória de forma. Dissertação, Instituto Politécnico de Bragança.

[4] Lobo, P. S., Almeida, J., Guerreiro, L. (2015). Semi-active damping device based on superelastic shape memory alloys. *Structures*, vol. 3, pp. 1-12.

[5] Qian, H., Li, H., Song, G. (2016). Experimental investigations of building structure with a superelastic shape memory alloy friction damper subject to seismic loads. *Smart Materials and Structures,* vol. 25.

[6] Li, H. N., Huang, Z., Fu, X., Li, G. (2018). A re-centering deformation-amplified shape memory alloy damper for mitigating seismic response of building structures. *Struct Control Health Monit*., vol. 25.

[7] Morais, J., Morais, P. G., Santos, C., Costa, A. C., Candeias, P. (2017). Shape memory alloy based dampers for earthquake response mitigation. *Procedia Structural Integrity*, vol. 5, pp. 705-712.

[8] Speicher, M. S., DesRoches, R., Leon, R. T., Investigation of an articulated quadrilateral bracing system utilizing shape memory alloys. *Journal of Constructional Steel Research*, vol. 130, pp. 65-78.

[9] Garafolo, N. G., McHugh, G. R. (2018). Mitigation of flutter vibration using embedded shape memory alloys. *Journal of Fluids and Structures*, vol. 76, pp. 592-605.

[10] Brinson, L. C. (1993). One-dimensional constitutive behavior of shape memory alloys: Thermomechanical derivation with non-constant material functions and redefined martensite internal variable. *Journal of Intelligent Material Systems and Structures*, vol. 4.

[11] Tanaka, K., Kobayashi, S., Sato, Y. (1986). Thermomechanics of transformation pseudoelasticity and shape memory effect in alloys. *International Journal of Plasticity*, vol. 2, pp. 59-72.

[12] Auricchio, F. (2001). A robust integration-algorithm for a finite-strain shape-memory-alloy superelastic model. *International Journal of Plasticity*, vol. 17, pp. 971-990.

[13] Pasquali, P. R. Z. (2008). Análise limite de estruturas através de uma formulação em elasticidade não-linear. Dissertação, Universidade Federal do Rio Grande do Sul.

[14] RAO, S. S. (2011). *Mechanical Vibrations*. Prentice Hall: Pearson.

[15] Kelly, S. G. (2000). *Fundamentals of Mechanical Vibrations*. Europe: McGraw Hill.

[16] Razavilar, R., Fathi, Al., Dardel, M., Hadi, J. A. (2018). Dynamic analysis of a shape memory alloy beam with pseudoelastic behavior. *Journal of Intelligent Material Systems and Structures*, vol. 115.

[17] Moraes, Y. J. O., Silva, A. A., Rodrigues, M. C., *et al* (2018). Dynamical analysis applied to passive control of vibrations in a structural model incorporating SMA-SE coil springs. *Advances in Materials Science and Engineering*.

[18] Tobushi, H., Iwanaga, H., Tanaka, *et al* (1992). Stress-strain-temperature relationships of TiNi shape memory alloy suitable for thermomechanical cycling. *JSME International Journal*, Series I, vol 35, issue 3.

[19] Wang, B. and Zhu, S. (2018). Cyclic tension-compression behavior of superelastic shape memory alloy bars with buckling-restrained devices. *Construction and Building Materials*, vol. 186, pp. 103-113.

[20] Toi, Y. and He, J. (2010). Dynamic and cyclic response simulation of shape memory alloy devices. *ICCSA 2010, Part III, Lecture Notes in Computer Science,* vol. 6018, pp. 498-510.

[21] Paiva, A. and Savi, M. A. (1999). Sobre os modelos constitutivos com cinética de transformação assumida para ligas com memoria de forma. *XV Congresso Brasileiro de Engenharia Mecânica*. Águas de Lindóia: UNICAMP.

[22] SHARCNET – Shared Hierarchical Academic Research Computing Network, 4.14. Shape memory alloy (SMA). https://www.sharcnet.ca/Software/Ansys/17.0/enus/help/ans_mat/smas.html. (03/11/2018)